


PAPER

[View Article Online](#)
[View Journal](#) | [View Issue](#)Cite this: *Mater. Adv.*, 2020,
1, 2994Temperature sensitive hydrogels cross-linked by magnetic LAPONITE[®] RD[®]: effects of particle magnetization†Nikolai I. Lebovka, * Yurii M. Samchenko, Liudmyla O. Kernosenko, Tatiana P. Poltoratska, Natalia O. Pasmurtseva, Igor E. Mamyshev and Vladimir A. Gigiberiya

This work discusses the synthesis and the properties of magnetite modified LAPONITE[®] RD platelets (Lap). Magnetized Lap (mLap) nanoparticles were synthesized by a co-precipitation method with different weight ratios, $X = \text{Fe}_3\text{O}_4/\text{Lap}$ (0–2). For characterization of the samples the particle size distributions and sedimentation behavior in an external magnetic field were studied. Temperature sensible hydrogels based on *N*-isopropylacrylamide cross-linked by mLap were synthesized. An increased aggregation of mLap particles in aqueous suspensions has been revealed, but all the systems demonstrated high sedimentation stability. Significant effects of the value of X on the rate of sedimentation mLap particles in magnetic fields and on the swelling ability of hydrogels have been revealed. For example at $X = 2$, an increase in swelling by ≈ 2.7 was observed as compared with the swelling of hydrogels based on pure Lap nanoparticles.

Received 7th September 2020,
Accepted 13th October 2020

DOI: 10.1039/d0ma00687d

rsc.li/materials-advances

Introduction

Polymeric hydrogels are composed of hydrophilic polymer networks filled with large amounts of water (it can be more than 90%). Due to their ability to absorb significant amounts of water and biological fluids, softness, porosity and elasticity, hydrogels resemble the tissues of the human body more than any other synthetic biomaterial.^{1,2} In recent decades, due to their high biocompatibility, polymeric hydrogels have been successfully used in medicine and pharmaceutical industries.^{3–5} They are considered as intelligent materials⁶ for manufacturing of soft contact lenses,⁷ devices for targeted delivery and sustained release of drugs,⁸ biosensors,⁹ anti-burn and hemostatic dressings,¹⁰ materials for tissue engineering and plastic surgery.¹¹

Nowadays great attention has been paid to polymeric hydrogels with stimuli responsiveness (pH, ionic strength, temperature, light, electric, magnetic fields, *etc.*).^{12–14} For example, pH-sensitive hydrogels containing carboxylic or amine functional groups can be used for controlled release of selectively adsorbed drugs.¹⁵

The very popular are hydrogels based on acrylic monomers cross-linked using different chemical linkers.^{16,17} At room

temperatures these temperature sensible hydrogels absorb a considerable amount of water and have an expanded hydrated conformation. However, under heating above ≈ 305 K they demonstrate transition into a compact dehydrated state.^{18,19} The transition temperature is close to the temperature of the human body and can be shifted to higher or lower temperatures by copolymerization with hydrophilic or hydrophobic monomers, respectively.¹⁹ This behaviour can be used to create a thermoregulatory drug delivery system, in particular photosensitizers.²⁰ The main disadvantages of such hydrogels are related to their low optical transparency, mechanical strength, low response rate and swelling ability in water.

These disadvantages can be avoided using the additive of platelets of LAPONITE[®] (Lap).²¹ Hydrogels cross-linked by Lap nanoparticles have exhibited extraordinary mechanical toughness, tensile moduli and tensile strengths²² that were almost proportional to the platelet content. Such hydrogels have great potential for the fabrication of flexible pressure and strain sensors.²³ The shape anisotropy of Lap nanoparticles and heterogeneity of surface charge distribution can lead to complex self-assembly and networking inside such systems.²⁴ Lap-doped hydrogels based on acrylamide,²⁵ acrylic acid,²⁶ *N*-isopropylacrylamide,²⁷ and dimethyl-acrylamide²⁸ have been already synthesized. As examples, Lap was used as an effective cross-linker for preparing the poly(*N,N*-dimethylaminoethyl methacrylate) based pH and temperature double-sensitive hydrogels with homogeneous distribution of the cross-link

Institute of Biocolloidal Chemistry named after F. D. Ovcharenko, NAS of Ukraine, 42, blvr. Vernadskogo, Kyiv 03142, Ukraine. E-mail: lebovka@gmail.com

† Electronic supplementary information (ESI) available: Experimental section and supplementary figures. See DOI: 10.1039/d0ma00687d



points along the gels.²⁹ Lap has been used as a cross-linker for preparation of stimuli-responsive hydrogels and cryogels based on poly(*N,N*-dimethylaminoethyl methacrylate-*co*-2-acrylamido-2-methyl propanosulfonic acid) copolymeric networks.³⁰ Lap based hydrogels demonstrated excellent mechanical strength that could be adjusted by controlling the content of Lap. Thermoresponsive hydrogel bioinks based on block copolymer poly(2-methyl-2-oxazoline)-*b*-poly(2-*n*-propyl-2-oxazine) and Lap were recently prepared.³¹ The materials demonstrated improved thermogelling and rheological properties beneficial for extrusion-based 3D printing.

Particularly, temperature sensitive hydrogels based on poly(*N*-isopropylacrylamide) (PNIPAAm) attract great attention as they exhibit a reversible volume phase transition at $T \approx 34^\circ\text{C}$ close to the physiological temperature range.³² The cross-linking of PNIPAAm by Lap allowed the preparation of hydrogels with high transparency, and excellent swelling and mechanical properties compared to chemically cross-linked hydrogels.³³ The strong interaction between silicate platelets and PNIPAAm chains was explained by a combination of ionic interactions and hydrogen bonding.²⁸ Recently, a technique for the preparation of anisotropic thermoresponsive hydrogels based on PNIPAAm cross-linked by Lap has been reported.³⁴ The hydrogels demonstrated anisotropic mechanical performance and could be deformed anisotropically in response to a temperature change. The content of Lap incorporated in PNIPAAm can affect the storage modulus, phase transition temperature and swelling/deswelling rates.³⁵

Application of magnetized Lap particles can improve the functionality of hydrogels. Different types of magnetite-covered clay nanoparticles *e.g.*, Fe_3O_4 -montmorillonite,³⁶ Fe_3O_4 -rectorite,³⁷ and Fe_3O_4 -Lap³⁸ were synthesized. Magnetic interactions are very effective in controlling the spatial distribution of colloidal particles³⁹ and, unlike electrostatic interactions, they can be carried out without direct contact between the medium and the field. The use of a magnetic field allows applying a number of strategies with various advantages to enhance the functional properties of hydrogels.⁴⁰ Recently, temperature sensitive hydrogels based on PNIPAAm cross-linked by magnetically modified Lap (mLap) nanoparticles have been synthesized.⁴¹ The weight ratio of Fe_3O_4 and Lap was fixed at $X = 1$. The structure of mLap was characterized by scanning electron microscopy and infrared spectroscopy. However, detailed studies on the effects of magnetization Lap platelets (value of X) and properties of temperature sensitive hydrogels supported by magnetized Lap platelets have not yet been performed.

This work discusses the synthesis and properties of magnetic Lap platelets (mLap) with different feed weight ratios $X = \text{Fe}_3\text{O}_4/\text{Lap}$ in the interval between 0 and 2. For characterization of the samples, particle size distribution and sedimentation of magnetic particles in an external magnetic field applied in a vertical direction were studied. The temperature-sensitive hydrogels based on poly(*N*-isopropylacrylamide) (PNIPAAm) physically cross-linked by mLap were synthesized. Their swelling was also discussed.

Materials and methods

Materials

LAPONITE[®] RD (Lap, Rockwood, Clay additives GmbH) is a synthetic clay of the general formula $\text{Si}_8\text{--Mg}_{5.45}\text{Li}_{0.4}\text{H}_4\text{O}_{24}\text{Na}_{0.7}$. Lap is composed of disk-shaped crystals with a thickness of $h \approx 1\text{ nm}$ (0.92 nm) and diameter of $d \approx 25\text{ nm}$. It has density of $\rho = 2.53\text{ g cm}^{-3}$ and its specific area can be theoretically estimated to be $S = 2/(\rho h) \approx 430\text{ m}^2\text{ g}^{-1}$. In aqueous media, Lap has a tendency to degrade (dissolve), particularly under acidic conditions.^{43–46} Increase in pH, and concentration of Lap as well as that of salt resulted in a stabilizing effect against degradation.⁴⁶ The faces are charged negatively and at pH 10, the edge surface is weakly positive.

Iron(II) sulfate heptahydrate $\text{FeSO}_4 \cdot 7\text{H}_2\text{O}$ (Merck, 99%), iron(III) chloride FeCl_3 (Merck, 98%), ammonium $\text{NH}_3 \cdot \text{H}_2\text{O}$ (Merck, 25%), tetrasodium pyrophosphate $\text{Na}_4\text{P}_2\text{O}_7$ (TSPP, Merck, 95%), ammonium persulfate $(\text{NH}_4)_2\text{S}_2\text{O}_8$, (APS, Sigma, 98%), *N,N,N',N'*-tetramethylethylenediamine, (TEMED, Merck, 99%), and tetrasodium pyrophosphate (TSPP, Merck) were used as received without further purification. *N*-Isopropylacrylamide, NIPAAm, (Sigma-Aldrich, 97%) was recrystallized from hexane and dried under vacuum. More details on the chemicals used in this paper are presented in ESI,[†] Table S1.

Synthesis procedures

Magnetic Fe_3O_4 /Lap particles. Magnetic Fe_3O_4 /Lap particles (mLap) with different Fe_3O_4 and Lap ratios $X (= \text{Fe}_3\text{O}_4/\text{Lap g g}^{-1})$ between 0 and 2 were synthesized using a co-precipitation method.^{38,47}

Initially, Lap was dispersed in distilled water degassed by N_2 at 20°C . The concentration of Lap was 1.5 wt% (hereinafter %). The suspension was carefully mixed for 10 min using an ultrasound clean bath operating at 25 kHz with a power of 140 W (Nitecore NFF01, China). A careful stirring procedure was applied for good exfoliation of Lap tactoids in water.^{24,48} Then, the temperature was increased up to 70°C , the solutions containing certain amounts of $\text{FeSO}_4 \cdot 7\text{H}_2\text{O}$ and FeCl_3 of distilled water were added to the suspension of Lap, and the mixtures were stirred at 250 rpm by using a magnetic stirrer (Heidolph MR 3004 S) in an N_2 atmosphere for 10 min. Ammonia solution ($\text{NH}_3 \cdot \text{H}_2\text{O}$) was added drop-wise to prepare iron oxides. The pH of the final mixture was about 10. The obtained mixtures were aged at 70°C for 2 hours. Finally, the mLap particles were separated from the aqueous suspension using a magnet. After magnetic separation the suspensions of mLap particles (1 : 1) were washed several times with distilled water. Commonly after the first three washings the suspension pH attained the neutral value pH 7. Then the samples were dried at room temperature until the final moisture content of $\leq 1\%$ and the obtained mLap particles were used for the preparation of thermosensitive NIPAA-based hydrogels.

The mLap synthesis procedure is schematically presented in Fig. 1a. It can be assumed that because of the high ion exchange capacity of Lap, the iron ions are adsorbed on Lap surfaces. It can result in the formation of nanomagnetite spots



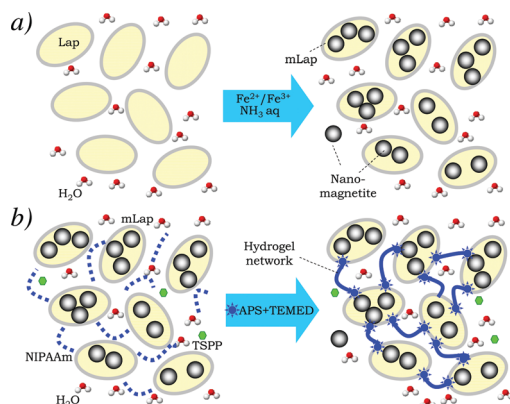


Fig. 1 Preparation schemes of magnetic Lap (mLap) nanoparticles (a) and temperature-sensitive hydrogels based on poly(*N*-isopropylacrylamide) (PNIPAAm) physically cross-linked by mLap (b). Structural formulae of NIPAAm, TSPP, APS and TEMED are presented in ESI† Table S1.

on the surface of Lap (Fig. 1a). However, formation of some quantity of Fe_3O_4 nanoparticles in partially exfoliated galleries of Lap and individual Fe_3O_4 nanoparticles cannot be excluded.

The interactions between Fe_3O_4 and Lap species in magnetized mLap samples were supported by a noticeable shift of the Fe–O vibration band of magnetite in FTIR spectra and changes in TGA traces (Fig. S1 and S2 in ESI†).

The previous SEM studies of Fe_3O_4 + Lap composites in powder state revealed the presence of spherical particles of 5–10 nm in size attributed to the formed structure of magnetite in magnetic composites.⁴¹

Temperature sensitive magnetic hydrogels. Temperature sensitive hydrogels based on NIPAAm were cross-linked using mLap particles at fixed Lap/NIPAAm = 0.5 ratio and different values of X . The synthesis procedure was similar to that described in ref. 27 and it is schematically presented in Fig. 1b. The gel formation can be explained by anchoring NIPAAm chains to the Lap platelets and decoration of their surfaces. The composite mLap powder (with different values of X) and NIPAAm were dispersed in aqueous TSPP solution and treated in an ultrasonic bath operating at 25 kHz with a power of 140 W (Nitecore NFF01, China) for 1 min. Then the components of the oxidation–reduction initiating system were added (aqueous solutions of APS and TEMED), the mixture was purged with N_2 for 3 min, and poured into the space between two glasses separated by spacers with a thickness of 0.7 mm. More details on the synthesis procedure are presented in ref. 41.

Methods. The particle size distributions were measured by a light scattering technique using a Mastersizer 3000 (Malvern Instruments, United Kingdom). Before these experiments the aqueous suspensions of mLap (0.3% weight to measure particle size distribution) were treated using an ultrasonic liquid processor *Sonicator* XL2020 (Misonix Inc., Japan, 500 W, 22 kHz) for 3 min.

The sedimentation stability of mLap aqueous suspensions in the absence and presence of external magnetic fields was evaluated by the spectrophotometric method using a photo-electrocolorimeter KFK-2MP (Zagorsky Optical-Mechanical

Plant, Russia) at a wavelength of 540 nm. The magnetic field was induced by a AlNiCo500 magnet ($50 \times 25 \times 8$ mm, residual flux density 1210 mT, Poland) placed at the bottom of the cuvette. The time dependence of optical transmission, $T_t(t)$, was measured.

The swelling ability S of hydrogels, defined as $S = m_s/m_d - 1$ (here, m_s , and m_d are the masses of the swollen (after 24 hours of swelling) and dry hydrogels, respectively) was studied in distilled water by the gravimetric method. The samples were weighed with an accuracy up to 10^{-4} g using an analytical balance “Axis” (Poland).

All measurements were conducted at approximately the same value, pH \approx 6.

Statistical analysis. Each experiment was repeated at least three times. The error bars, presented on the figures, correspond to the standard deviations. One-way analysis of variance (ANOVA) was used to determine significant differences ($p < 0.05$) among the samples with the help of an OriginPro 8.5 (developed by OriginLab Corporation, Northampton, USA). Differences between means were detected using Tukey's test.

Results and discussion

Fig. 2 shows different examples of the separation of mLap aqueous suspensions by interaction with a magnet. The preliminary studies have shown that there exists a certain critical threshold of X (≈ 0.05) above which the effects of magnet on the separation of the suspension become observable. However, for $X \geq 0.125$ after relatively long time ($t \approx 15$ min), practically all mLap particles can be separated from the aqueous suspension using a magnet.

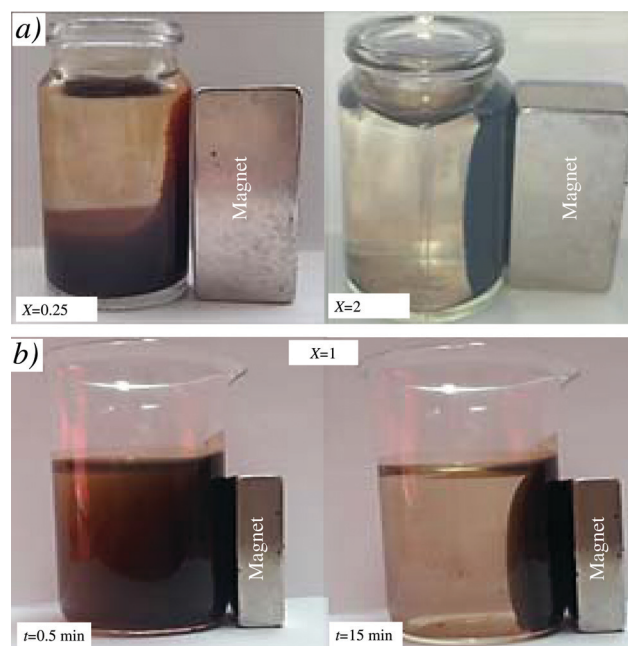


Fig. 2 Different examples of the separation of mLap aqueous suspensions by interaction with a magnet for weight ratios of Fe_3O_4 and Lap $X = 0.25$ and $X = 2$ ($t = 15$ min) (a) and $X = 1$ for $t = 0.5$ and $t = 15$ min (b).



Fig. 3 shows the examples of particle size distribution functions $f(d)$ for samples with different contents of magnetite X ($\text{Fe}_3\text{O}_4/\text{Lap}$). For the highest content of magnetite ($X = 2$), the largest aggregates of mLap nanoparticles were formed with the peak of $f(d)$ function located at $d_m \approx 361$ nm. A decrease in X resulted in a decrease in d_m and finally, for the smallest content of magnetite ($X = 0.125$) the peak of $f(d)$ function was located at $d_m \approx 85$ nm. It corresponded to the formation of aggregates of several mLap nanoparticles. Inset in Fig. 3 shows the $d_m(X)$ dependence.

Therefore, the coverage of Lap particles by nanomagnetite can cause formation of relatively large aggregates of magnetic particles. Moreover, the heterocoagulation between individual Lap platelets and magnetite can also result in the formation of large aggregates. This heterocoagulation may be supported by differences in surfaces charges of Lap⁴⁹ and nanomagnetite⁵⁰ particles. Such heterocoagulation was observed in the sedimentation behavior in magnetic fields for mechanical mixtures of nanometric magnetite and micron-sized sodium montmorillonite particles.³⁶

Nevertheless all these aggregates in mLap suspensions were relatively small and overall, the suspensions preserved their sedimentation stability owing to the thermal energy.

The magnetic properties of the magnetized mLap nanoparticles were investigated indirectly using sedimentation analysis. The effects of a magnetic field on sedimentation stability can be illustrated by changes in the optical transmission of the suspension. Similar experiments were performed for mixtures of nanomagnetite and sodium montmorillonite.³⁶

Examples of time dependences of the normalized optical transmission $T_r^*(t) = T_r(t)/T_r^m$ (here T_r^m is a maximum (saturation) transmission at long time of sedimentation) for different X are presented in Fig. 4a. The presented dependencies evidenced the existence of a long delay time before starting sedimentation. The derivative $dT_r^*(t)/d \log t$ can be used for the calculation of the characteristic sedimentation time τ (Fig. 4b).

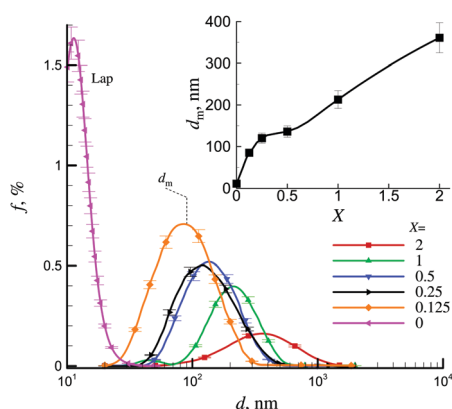


Fig. 3 Particle size distribution functions $f(d)$ for 0.3% aqueous suspensions of Lap and mLap at different values of X ($=\text{Fe}_3\text{O}_4/\text{Lap}$). Inset shows the position of peak maximum d_m versus X . For particular case of $X = 1$, the observed bimodal size distribution (with an insignificant peak at $d \approx 50$ nm) can reflect the presence of some inhomogeneity of mLap particles.

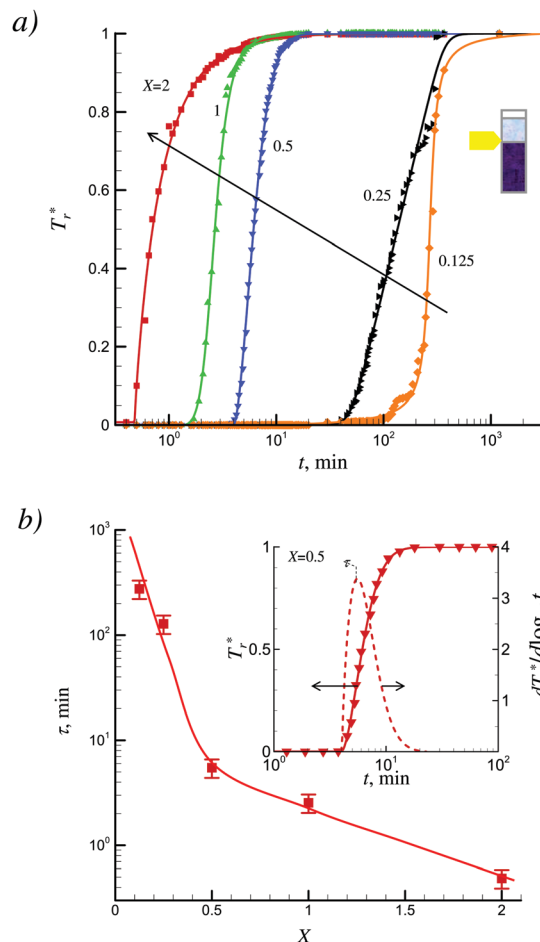


Fig. 4 Normalized optical transmission T_r^* versus the deposition time t in an external magnetic field for suspensions of mLap at different values of X ($=\text{Fe}_3\text{O}_4/\text{Lap}$) (a) and characteristic sedimentation time τ versus the X (b). Inset in (b) presents examples of $T_r^*(t)$ and derivative $dT_r^*(t)/d \log t$ for a sample with $X = 0.5$ that was used for the derivation of τ .

Note that in the absence of a magnetic field, the suspensions of mLap were rather stable and very slow sedimentation for several days was observed. In the presence of a magnetic field the sedimentation was more accelerated at high values of X . For example, the characteristic sedimentation time was ≈ 4.6 hours at $X = 0.125$ and decreased up to ≈ 30 s at $X = 2$.

Such a significant effect of the magnetic field on sedimentation can reflect a direct effect of magnetic field on the magnetic particles and formation of big flocculi in the suspension due to the dipole-dipole magnetic attractions between magnetite-covered clay platelets.³⁶ The noticeable retardation in sedimentation for X below 0.5 (Fig. 4b) can reflect the high stability of suspensions for small-sized aggregates (< 100 nm, Fig. 3) and weakening of the magnetic field effects on the deposition processes.

Stimuli-sensitive hydrogels (e.g., chemical, pH and temperature sensitive) have attracted considerable attention in the pharmaceutical field due to the possibility of their applications as a biosensor and in the drug release process.^{3,51} Physical cross-linking of hydrogels by magnetically modified Lap platelets



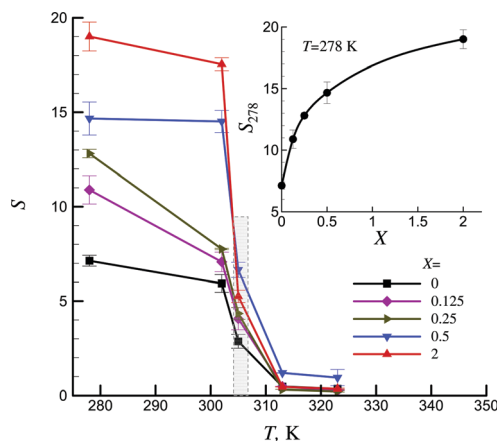


Fig. 5 Temperature dependence of the swelling degree of NIPAA-mLap (Lap) S at different values of X ($=\text{Fe}_3\text{O}_4/\text{Lap}$). In all hydrogels the same ratio Lap/NIPAAm = 0.5 was used. The time of swelling at $T = 277$ K was 24 hours. Inset shows the maximum swelling ratio S_{278} at $T = 278$ K versus X dependence.

can open new perspectives for supplementary physical stimuli in these promising applications.

The studied physically cross-linked by Lap platelet hydrogel is negative temperature-sensitive;⁵² it has a lower critical solution temperature and contracts upon heating in the range of 304–308 K (dashed area in Fig. 5). It reflects the ability of the system to exhibit hydrophilic nature at low temperatures and hydrophobic nature above some critical temperatures. Such hydrogels can be used for temperature-modulated drug release by bulk squeezing and surface regulation.⁵³ Magnetic modification of Lap significantly affected the hydrophilic properties of NIPAA-based temperature sensitive hydrogels. It should be noted that magnetic modification practically has no effect on the transition temperature.

Inset in Fig. 5 shows that magnetization of Lap led to an increase in the swelling ability in the low temperature range. For example, at $T = 278$ K and $X = 2$ an increase by ≈ 2.7 was observed as compared with the swelling ability of hydrogels based on pure Lap nanoparticles. Therefore, the degree of magnetization of Lap particles can significantly affect the hydrophilic properties of the hydrogel.

The swelling behavior of magnetic hydrogels can reflect the mechanism of hydrogel formation and nature of magnetic nanoparticles. For example, in magnetic alginate hydrogels (consisting of magnetic iron particles embedded within the alginate network), prepared by a special two-step protocol, the swelling capacity was not affected by the presence or content of the magnetic particles.⁵⁴ This was explained by the insignificant effects of magnetic particles on the porosity of the hydrogels. Similar insignificant effects of magnetic particles on the swelling ability of poly(2-oxazoline)-based magnetic hydrogels were also observed.⁵⁵ However, the mechanism of Lap magnetization on the swelling of magnetic hydrogels is not completely clear. It can be speculated that the observed effects can reflect the significant effects of Lap magnetisation on the structure and porosity of hydrogels.

Note that the physical cross-linking supported by silicate platelets enhance the mechanical properties of the hydrogels.²¹ Covering Lap by nanomagnetite and formation of aggregates of mLap can affect the rigidity of the polymeric chains without breakdown of the total networks. Therefore, more thorough studies are desirable in future to elucidate the effects of mLap on mechanical and rheological properties of magnetic hydrogels.

Conclusions

Hybrid magnetic particles based on the platelets of Lap (mLap particles) covered by magnetite with different weight ratios $X = \text{Fe}_3\text{O}_4/\text{Lap}$ ($X = 0$ – 2) have been prepared and used for the synthesis of the temperature-sensitive hydrogels (PNIPAAm) physically cross-linked by mLap. The analysis of the particle size distributions revealed an increased aggregation of mLap particles in aqueous suspensions, but all the systems demonstrated high sedimentation stability. Sedimentation behavior in magnetic fields of magnetite-covered Lap particles evidenced the presence of a significant effect of the value of X on the rate of sedimentation. Moreover, temperature sensitive hydrogels cross-linked by mLap particles demonstrated the presence of a significant increase in the swelling ability. For example at $X = 2$ an increase by ≈ 2.7 was observed as compared with the swelling ability of hydrogels based on pure Lap nanoparticles.

Conflicts of interest

There are no conflicts to declare.

Acknowledgements

We acknowledge funding from the National Academy of Sciences of Ukraine, Projects 7/9/3-f-4-1230-2020 #0120U100226, # 0120U102372/20-N, and #0120U102343/20-N.

Notes and references

- Q. Chai, Y. Jiao and X. Yu, *Gels*, 2017, **3**, 6.
- J. Fu and M. in het Panhuis, *J. Mater. Chem. B*, 2019, **7**, 1523–1525.
- N. A. Peppas, *Hydrogels in medicine and pharmacy: fundamentals*, CRC press, 2019, vol. 1.
- S. Rafeian, H. Mirzadeh, H. Mahdavi and M. E. Masoumi, *Sci. Eng. Compos. Mater.*, 2019, **26**, 154–174.
- H. Chang, C. Li, R. Huang, R. Su, W. Qi and Z. He, *J. Mater. Chem. B*, 2019, **7**, 2899–2910.
- M. Mahinroosta, Z. J. Farsangi, A. Allahverdi and Z. Shakoori, *Mater. today Chem.*, 2018, **8**, 42–55.
- O. Wichterle and D. Lim, *Nature*, 1960, **185**, 117–118.
- R. Narayanaswamy and V. P. Torchilin, *Molecules*, 2019, **24**, 603.
- X. Yu, Y. Jiao and Q. Chai, *Nano LIFE*, 2016, **6**, 1642001.
- R. Z. Murray, Z. E. West, A. J. Cowin and B. L. Farrugia, *Burn. trauma*, 2019, **7**, 2.



- 11 J. M. Shapiro and M. L. Oyen, *JOM*, 2013, **65**, 505–516.
- 12 S. Gao, G. Tang, D. Hua, R. Xiong, J. Han, S. Jiang, Q. Zhang and C. Huang, *J. Mater. Chem. B*, 2019, **7**, 709–729.
- 13 B. S. Gomes, P. M. Mendes and Q. Li, in *Functional Organic and Hybrid Nanostructured Materials*, ed. Q. Li, John Wiley & Sons, Inc., Hoboken, NJ, USA, 2018, pp. 203–243.
- 14 J. Hoque, N. Sangaj and S. Varghese, *Macromol. Biosci.*, 2019, **19**, 1800259.
- 15 R. Kouser, A. Vashist, M. Zafaryab, M. A. Rizvi and S. Ahmad, *ACS Appl. Bio Mater.*, 2018, **1**, 1810–1822.
- 16 N. Shah and K. Patel, *J. Pharm. Sci. Biosci. Res.*, 2014, **4**, 114–120.
- 17 D. Qureshi, S. K. Nayak, S. Maji, A. Anis, D. Kim and K. Pal, *Eur. Polym. J.*, 2019, **120**, 109220.
- 18 N. A. Platé, T. L. Lebedeva and L. I. Valuev, *Polym. J.*, 1999, **31**, 21.
- 19 U. G. Spizzirri, I. Altimari, F. Puoci, O. I. Parisi, F. Iemma and N. Picci, *Carbohydr. Polym.*, 2011, **84**, 517–523.
- 20 Y. Samchenko, G. Dolinsky, N. Pasmurtseva, T. Poltoratskaya, Z. Ulberg and M. Gamalia, *Nauk. Sci. Notes. - Chem. Sci. Technol.*, 2015, **170**, 34–39.
- 21 K. Haraguchi, T. Takehisa and S. Fan, *Macromolecules*, 2002, **35**, 10162–10171.
- 22 J. Yang, S. Liu, Y. Xiao, G. Gao, Y. Sun, Q. Guo, J. Wu and J. Fu, *J. Mater. Chem. B*, 2016, **4**, 1733–1739.
- 23 Z. Wang, Y. Cong and J. Fu, *J. Mater. Chem. B*, 2020, **8**, 3437–3459.
- 24 N. Lebovka, L. Lisetski and L. A. Bulavin, in *Modern Problems of the Physics of Liquid Systems*, ed. L. Bulavin and L. Xu, Springer Nature, Cham, Switzerland AG, 2019, pp. 137–164.
- 25 O. Okay and W. Oppermann, *Macromolecules*, 2007, **40**, 3378–3387.
- 26 H. Li, R. Gu, S. Xu, A. Abudurman and J. Wang, *Appl. Clay Sci.*, 2014, **101**, 335–338.
- 27 M. Shibayama, J. Suda, T. Karino, S. Okabe, T. Takehisa and K. Haraguchi, *Macromolecules*, 2004, **37**, 9606–9612.
- 28 K. Haraguchi, R. Farnworth, A. Ohbayashi and T. Takehisa, *Macromolecules*, 2003, **36**, 5732–5741.
- 29 Y. Chen, W. Xu, Y. Xiong, C. Peng, W. Liu, G. Zeng and Y. Peng, *J. Mater. Res.*, 2013, **28**, 1394–1404.
- 30 T. Boyacı and N. Orakdogan, *Appl. Clay Sci.*, 2016, **121**, 162–173.
- 31 C. Hu, L. Hahn, M. Yang, A. Altmann, P. Stahlhut, J. Groll and R. Luxenhofer, *J. Mater. Sci.*, 2020, 1–15.
- 32 K. László, K. Kosik and E. Geissler, *Macromolecules*, 2004, **37**, 10067–10072.
- 33 S. S. Das, K. Hussain, S. Singh, A. Hussain, A. Faruk and M. Tebyetekerwa, *et al.*, *Curr. Pharm. Des.*, 2019, **25**, 424–443.
- 34 L. Chen, Q. Wu, J. Zhang, T. Zhao, X. Jin and M. Liu, *Polymer*, 2020, **192**, 122309.
- 35 I. Mirković, M. S. Nikolić, S. Ostojić, J. Maletaškić, Z. Petrović and J. Djonlajić, *J. Serb. Chem. Soc.*, 2020, **85**(9), 1197–1221.
- 36 C. Galindo-Gonzalez, J. De Vicente, M. M. Ramos-Tejada, M. T. Lopez-Lopez, F. Gonzalez-Caballero and J. D. G. Duran, *Langmuir*, 2005, **21**, 4410–4419.
- 37 D. Wu, P. Zheng, P. R. Chang and X. Ma, *Chem. Eng. J.*, 2011, **174**, 489–494.
- 38 G. R. Mahdavinia, Z. Rahmani, A. Mosallanezhad, S. Karami and M. Shahriari, *Desalin. Water Treat.*, 2016, **57**, 20582–20596.
- 39 K. Komae, B. Yellen, G. Friedman and N. Dan, *J. Colloid Interface Sci.*, 2006, **297**, 407–411.
- 40 W. Shi, J. Huang, R. Fang and M. Liu, *ACS Appl. Mater. Interfaces*, 2020, **12**, 5177–5194.
- 41 O. Goncharuk, Y. Samchenko, D. Sternik, L. Kernosenko, T. Poltorats'ka, N. Pasmurtseva, M. Abramov, E. Pakhlov and A. Derylo-Marczewska, *Appl. Nanosci.*, 2020, DOI: 10.1007/s13204-020-01388-w.
- 42 E. S. H. Leach, A. Hopkinson, K. Franklin and J. S. van Duijneveldt, *Langmuir*, 2005, **21**, 3821–3830.
- 43 A. Mourchid and P. Levitz, *Phys. Rev. E: Stat. Phys., Plasmas, Fluids, Relat. Interdiscip. Top.*, 1998, **57**, R4887.
- 44 S. Jatav and Y. M. Joshi, *Appl. Clay Sci.*, 2014, **97**, 72–77.
- 45 D. W. Thompson and J. T. Butterworth, *J. Colloid Interface Sci.*, 1992, **151**, 236–243.
- 46 R. P. Mohanty and Y. M. Joshi, *Appl. Clay Sci.*, 2016, **119**, 243–248.
- 47 G. R. Mahdavinia, M. Soleymani, M. Sabzi, H. Azimi and Z. Atlasi, *J. Environ. Chem. Eng.*, 2017, **5**, 2617–2630.
- 48 S. Ali and R. Bandyopadhyay, *Langmuir*, 2013, **29**, 12663–12669.
- 49 M. Manilo, N. Lebovka and S. Barany, *Colloids Surf., A*, 2014, **462**, 211–216.
- 50 M. Manilo, S. Netreba, V. Prokopenko, N. Lebovka and S. Barany, *Colloids Surf., A*, 2016, **506**, 291–297.
- 51 Z. Qiao, M. Cao, K. Michels, L. Hoffman and H.-F. Ji, *Polym. Rev.*, 2019, **60**(3), 1–22.
- 52 N. A. Peppas, P. Bures, W. S. Leobandung and H. Ichikawa, *Eur. J. Pharm. Biopharm.*, 2000, **50**, 27–46.
- 53 A. S. Hoffman, *Adv. Drug Delivery Rev.*, 2012, **64**, 18–23.
- 54 C. Gila-Vilchez, A. B. Bonhome-Espinosa, P. Kuzhir, A. Zubarev, J. D. G. Duran and M. T. Lopez-Lopez, *J. Rheol.*, 2018, **62**, 1083–1096.
- 55 M. Cvek, A. Zahoranova, M. Mrlik, P. Sramkova, A. Minarik and M. Sedlacik, *Colloids Surf., B*, 2020, 110912.

